Open access • Journal Article • DOI:10.1061/(ASCE)MT.1943-5533.0001573

Impact of Lime, Cement, and Clay Treatments on the Internal Erosion of Compacted Soils — Source link

Abdelwadoud Mehenni, Olivier Cuisinier, Farimah Masrouri

Institutions: University of Lorraine

Published on: 24 Mar 2016 - Journal of Materials in Civil Engineering (American Society of Civil Engineers)

Topics: Internal erosion, Silt, Soil stabilization, Erosion and Cement

Impact of Lime, Cement, and Clay Treatments on the Internal Erosion of Compacted Soils

Abdelwadoud Mehenni, Olivier Cuisinier, Farimah Masrouri

To cite this version:

Abdelwadoud Mehenni, Olivier Cuisinier, Farimah Masrouri. Impact of Lime, Cement, and Clay Treatments on the Internal Erosion of Compacted Soils. Journal of Materials in Civil Engineering, American Society of Civil Engineers, 2016, 28 (9), pp.04016071. 10.1061/(ASCE)MT.1943-5533.0001573 . hal-01409044

Impact of lime, cement and clay treatments on the internal erosion of compacted soils

Author 1: Abdelwadoud Mehenni [1,2]
Affiliation 1: PhD Student - Laboratoire d'Energétique et de Mécanique Théorique et Appliquée, UMR 7563 CNRS - Université de Lorraine
2 rue du Doyen Marcel Roubault
TSA 70605
54518 VANDOEUVRE LES NANCY
France

Affiliation 2: DTP - Bouygues Construction
Challenger, 1 avenue Eugène Freyssinet
Guyancourt
78061 St-Quentin-en-Yvelines
France

a.mehenni@bouygues-construction.com

Author 2: Olivier Cuisinier
Affiliation: Associate Professor - Laboratoire d'Energétique et de Mécanique Théorique et Appliquée, UMR 7563 CNRS - Université de Lorraine
2 rue du Doyen Marcel Roubault
TSA 70605
54518 VANDOEUVRE LES NANCY
France

olivier.cuisinier@univ-lorraine.fr

Author 3: Farimah Masrouri
Affiliation: Professor - Laboratoire d'Energétique et de Mécanique Théorique et Appliquée, UMR 7563 CNRS - Université de Lorraine
2 rue du Doyen Marcel Roubault
TSA 70605
54518 VANDOEUVRE LES NANCY
France

farimah.masrouri@univ-lorraine.fr

Keywords

Soil stabilization, internal erosion, lime, cement, clay treatment

Abstract

The aim of this paper is to study the impact of certain soil treatments on the internal erosion characteristics of treated compacted silt. The experiments measured the internal erosion using the hole erosion test (HET). This study aims to describe the effects of clay, lime and cement soil treatments on the internal erosion, specifically with regard to the amount of treatment used and the curing time. The internal erosion resistance was quantified by the coefficient of soil erosion and the critical shear stress. The results demonstrated that clay treatment could reduce the coefficient of soil erosion depending on the nature and percentage of clay added to the soil. The results also showed that lime and cement treatment primarily increased the critical shear stress of the tested silt. This increase was higher with cement treatment and was dependent on the amount of the added product. The impact of the curing time (up to 30 days) on the evolution of the erosion characteristics was not relevant for the lime-treated silt, whereas that of the cement-treated silt was dependent on the amount of cement added to the soil.

Introduction

Soil treatment with different types of clays, lime or cement is widely used in geotechnical engineering to improve soil characteristics and thus achieve a higher design strength, elastic modulus, and lower hydraulic conductivity, among other features. The main effects of these treatments on the geotechnical characteristics of compacted soils are relatively well known.

Clayey soils are often used as treatment product specifically to reduce the hydraulic conductivity of soils in order to reach a target design. The reduction of the hydraulic conductivity depends on the percentage and the nature of the clayey soil employed (e.g., Sivapullaiah et al., 2000, Chapuis, 2002). Several authors (e.g., Eades and Grim 1966, Brandl, 1981, Bell 1996) showed that lime treatment improves mainly the soil workability as well as the soil strength. Lime effects on the hydraulic conductivity of soils depend on the compaction conditions (McCallister and Petry 1991, Le Runigo et al., 2009, Cuisinier et al., 2011). Several studies showed the enhancement of mechanical characteristics of soils after cement treatment (e.g., Al-Amoudi 2002, Sariosseiri and Muhunthan 2009). The addition of cement is often related to a decrease of the hydraulic conductivity. However some authors (e.g., Bellezza and Fratalocchi, 2006) showed that the evolution of the hydraulic conductivity is mainly related to the nature of soil, and may increase or decrease after treatment.

Nevertheless, using compacted treated soils to build hydraulic earth structures (e.g., earth dams, levees, water retaining structures) raises some specific issues. Several objectives must be met simultaneously; specifically, low permeability and the overall stability of the earth structure are paramount. Moreover, these structures can be affected by different internal or external erosion phenomena. Erosion may affect soils, reducing the life of the structure or even leading to its destruction. Soil treatment with clays, lime or cement could be of interest to increase the strength and reduce soil erodibility, extending the service life of an earth structure. Therefore, the impact of these common treatments on erosion characteristics must be determined. After the description of the erosion process and its experimental characterization, a literature review on the effects of treatments on the internal erosion characteristics is presented.

Background

Erosion phenomena occurring on hydraulic earth structures can be classified into two categories: external erosion and internal erosion. External erosion concerns the outer surfaces of structures, whereas internal erosion occurs within the body of the structure. This study is focused on piping, which is an internal erosion mechanism. According to Fell et al. (2003), the process of internal erosion and piping can be divided into four phases: the initiation of erosion on a concentrated leak, the continuation of erosion, the progression of erosion by the enlargement of the concentrated leak to form a pipe, and the formation of a breach leading to the destruction of the structure.

To study internal erosion and piping, Wan and Fell (2002, 2004) developed the hole erosion test (HET), which was derived from other experimental erosion devices, such as the pinhole test (Sherard et al., 1976; ASTM D-4647), the drill hole test (Lefebvre et al., 1985 and Rohan et al., 1986), and the flow pump test (Reddi et al., 2000). The HET characterizes the behavior of soils only once a pipe is completely formed. The test does not allow for the study of the initial phase of the internal erosion process (i.e., the formation of the pipe in the soil). In fact, in the HET, a preformed hole in a soil sample is created to simulate a pipe; erosion of the pipe is then studied by subjecting the hole to a flow of water. The growth of the diameter of the hole is monitored by measuring hydraulic parameters (i.e., the pressure drop between the areas upstream and downstream of the sample and the flow through the hole). The results determine the empirical erosion law of the material, which can be expressed as follows:

$$\dot{\varepsilon} = k_{er} \, (\tau - \tau_c) \qquad (1)$$

where:

$\dot{\varepsilon}$ is the erosion rate per unit surface area of the hole at time t (kg/s/m^2),

τ is the hydraulic shear stress along the hole at time t (Pa),

k_{er} is the coefficient of soil erosion (s/m),

τ_c is the critical shear stress (Pa).

The HET yields two parameters that characterize the soil erosion behavior: *i)* the critical shear stress τ_c, corresponding to the minimum shear stress necessary to initiate the departure of soil particles; and *ii)* the coefficient of soil erosion k_{er}, which expresses the erosion rate during the erosion process.

To compute $\dot{\varepsilon}$ and τ, it is necessary to determine the variation of the diameter of the hole during the test; several assumptions are made following this measurement. It is assumed that erosion occurs on a uniform circular cross section along the length of the soil sample during the test. Wan and Fell (2004) proposed a method to determine the growth of the hole diameter during erosion based on the friction factor. This method required the determination of the final hole diameter after erosion, which is typically difficult to evaluate because the final shape of the hole is often irregular. Wan and Fell (2004) assumed that the friction factor in laminar or turbulent flow varies linearly with time. Two problems with this approach can be noted: 1) during the drilling step, the hole is disturbed, and thus, the initial friction factor used in the calculations is not representative of the real situation; and 2) the hypothesis of the linear variation of the friction factor on the hole during the test is not realistic (Haghighi et al., 2013). Another method uses the turbidity signal to compute the growth of the hole diameter during the test (Pham, 2008; Indraratna et al., 2009; Benahmed and Bonelli, 2012; Haghighi et al., 2013).

To classify soils by their resistance to internal erosion, authors often use the method proposed by Wan and Fell (2004), which is based on k_{er}. The Erosion Rate Index is calculated as *ERI* =

-log(k_{er}), and soils are classified by extremely rapid erosion (1) to extremely slow erosion (6), as shown in Table 1. However, this method does not consider τ_c, which qualifies the shear stress needed to initiate soil erosion along the pipe; this parameter is not included because the HET does not yield good repeatability of τ_c (Wan and Fell, 2002). Indeed, for specimens prepared under the same conditions, different studies indicated that both k_{er} and τ_c might vary from one test to another for the same soil. k_{er} can vary by a factor of 2 (e.g., Wan and Fell, 2002; Farrar et al., 2007), whereas τ_c may vary by a factor of more than 10 (e.g., Wan and Fell, 2002). The use of the *ERI* allows for the classification of different samples of the same soil in the same erosion group even if k_{er} varies from one test to another. Another method to overcome these repeatability issues is to use all results for $\dot{\varepsilon}$ and τ_c obtained from several specimens, prepared under the same conditions, to determine a unique erosion law (Pham, 2008; Haghighi, 2012).

In the last decade, several optimizations were made on the HET to allow for more control of the hydraulic parameters, such as the hydraulic pressure drop across the sample or the water flow rate (Pham, 2008; Indraratna et al., 2009; Whal, 2010; Benahmed and Bonelli, 2012; Luthi et al., 2012; Haghighi et al., 2013).

The HET was used to assess the impact of the compaction parameters (i.e., the initial water content, initial dry density and compaction energy) on the erodibility of compacted soils. Attom (2012) showed that at the same initial dry density, soils exhibit a higher *ERI* if they are compacted on the wet side of optimum. This observation has been confirmed by Wan and Fell (2002) and Lim (2006). The increase in the initial dry density of soil induces a higher *ERI* (Wan and Fell, 2002; Lim, 2006) and a higher τ_c (Benahmed and Bonelli, 2012). For compacted soils, the effects of the initial dry density, on increasing the *ERI,* are also related to the initial water content; the increase of the *ERI* is more pronounced on the dry side of optimum (Attom, 2012). Wahl (2010) and Attom (2012) have also shown that along the compaction curve, the highest *ERI* values are obtained for coupled values of the optimum initial water content and maximum dry density.

The percentage of clay particles can modify the internal erosion resistance of soils. Several authors showed that increasing the clay percentage induces a higher τ_c and lower k_{er} (Bennabi et al., 2012; Benahmed and Bonelli, 2012; Haghighi et al., 2013).

A limited number of studies considered the improvement of soil internal erosion characteristics by lime or cement treatment. To study the internal erosion of a specific soil, it is necessary to use a device capable of applying the necessary inlet pressure and hence the necessary pressure drop across the soil sample required to initiate the erosion of the studied soil. However, the existing devices are not convenient to fully characterize the impact of these treatments on erodibility due to technical limitations. In fact, the study of erosion in treated soils requires a high level of applied hydraulic shear stress that few devices can provide. Chevalier et al. (2012) showed that a 2% lime-treatment of silt can increase τ_c by a factor of at least 4. Herrier et al. (2012) studied a 2% lime-treated soil with a curing time of 14 days and observed that τ_c increased by a factor of 20, whereas k_{er} was reduced by a factor of 10. Indraratna et al. (2009) worked on silty sand treated with cement with a τ_c near zero before treatment; they showed that treatment with 3% cement increased τ_c by up to 50 Pa and decreased the k_{er} by two orders of magnitude. Additionally, they found that the decrease in erosion by cement treatment is directly related to the percentage of cement added to the soil.

Thus, the literature has shown that the HET could be a convenient method to quantify soil erodibility. Furthermore, treatment with clays, lime or cement could reduce soil erodibility. However, the limited data available did not provide a sufficient amount of information regarding the impact of clay treatment on silty soils or the impact of lime and cement treatments, the curing time and the percentage of admixture.

The main focus of this study is to investigate the impact of soil treatments on erosion characteristics. A new enhanced HET device was created to quantify the effects of different treatments. In the following sections, the testing procedures and theoretical models are presented, and the modifications produced by the treatments are discussed.

Materials and experimental setup

In this section, details regarding the tested materials and experimental setup are presented.

Materials

The studied soil was a silty soil from northern France; Table 2 summarizes the main physical and geotechnical properties of the soil. Four types of commonly used treatment products were considered: kaolinite (2 and 9%), bentonite (2%), quicklime (1 and 3%) and cement (3 and 6%). These percentages refer to the quantity of the product calculated on a dry soil weight basis. These choices were made based on usual field uses of these treatment products in France (SETRA-LCPC, 2000). The bentonite was sodium smectite clay. The lime used in this study contained 94% of quicklime (CaO). The category of the cement was CEM II (i.e., 65% of clinker, 35% of limestone and fly ash).

Specimen preparation

First, the compaction characteristics of the different mixtures were determined. For specimen preparation, the water content of the soil was adjusted to the desired water content for compaction. After a storage period of 24 h, during which the moisture content homogenized, the soil and treatment product were thoroughly mixed. When the lime treatment was added, the mixture was left for 1 h in an airtight container before compaction. When the cement treatment was used, compaction was carried out within a few minutes (maximum of 30 min) after treatment to account for the setting time of the cement. When clay treatments were used, no specific time was needed between the mixing and compaction; the mixture was statically compacted in the cell test to the target dry density. When a curing period prior to testing was required, the compacted samples were wrapped in plastic sheets and kept at 20.0 ± 1.5°C to prevent any water loss. The compaction characteristic curves were determined for each type and percentage of treatment according to the standard ASTM-D 698; the results of these experiments are summarized in Table 3.

Experimental strategy

Several authors (e.g., Mitchell et al. 1965; Benson and Daniel 1990; Watabe et al. 2000) showed that soil hydraulic conductivity reaches its minimum value on the wet side of optimum; thus, the investigations were focused on one specific compaction state for each treatment and each percentage. This state was defined by $w = w_{\mathrm{OMC}+3\%}$ and $\rho_d = 0.96\ \rho_{\mathrm{dmax}}$, depending on the nature and percentage of each treatment, where w is the compaction moisture content (%), w_{OMC} is the optimum moisture content (%), ρ_d is the dry density (Mg/m^3) and ρ_{dmax} is the maximum dry density (Mg/m^3) (Table 3). The soil, untreated and treated, was statically compacted directly in the cell mold. After treatment and compaction, the soil specimens were sealed in airtight bags and cured at 20°C for different periods (e.g., 0, 7, and 30 days) before starting the erosion tests.

Experimental procedures

In this section, the enhanced HET device, test procedure and theoretical calculation methods are described.

HET device

An enhanced HET device was developed to measure the internal erosion of the compacted treated soil specimens. This device included several optimizations that allowed for the application of a high inlet pressure, producing a large pressure drop across the sample and hence a high hydraulic shear stress along the hole.

Major improvements were made to the pressure system: the water pressure at the inlet of sample was applied with a special air-water reservoir; an electromechanically operated valve controlled the air flow in the air-water reservoir during the experiment; the inlet pressure was controlled by a sensor at the entrance of the sample; and the water pressure was also measured at the outlet of the sample. The maximum inlet pressure exceeded 650 kPa, producing the necessary pressure drop of 650 kPa between the flows upstream and downstream of the soil samples.

Other optimizations were made to the configuration of the testing cell. A detailed view of the testing cell is provided in Figure 1. The soil samples were strongly held within the testing device from both sides. This prevented any loss of pressure and water leakage and also allowed for better holding of the soil specimen during the test under the large pressure drops.

The water flow was measured with an ultrasonic flowmeter and ranged from 0 to 1.4 L/s. A turbidimeter was connected to the outlet of the test cell to measure the effluent turbidity to determine the diameter of the hole during the test.

The initial diameter of the hole in the sample was between 3 and 6 mm. The tested samples were cylindrical, with a diameter of 70 mm and a length between 70 and 150 mm. When using a sample of 70 mm length and an initial hole of 6 mm, the device allowed for the application of a hydraulic shear stress of approximately 10,000 Pa (calculated with equation 6).

Test procedure

The initial hole was made by drilling into the specimen center; the specimen was then placed in the testing cell. Saturation of the whole system ensured that no air bubbles were trapped inside the cell or pipes; this saturation was established under a low flow while the vent valves were open. The erosion test was conducted by controlling and monitoring hydraulic parameters (i.e., the pressure applied to the sample, the pressure drop between the upstream and downstream of sample, and the flow through the hole).

In the literature, three different methods were used depending on which hydraulic parameter was applied and controlled during the test: i) applying a constant pressure at the upstream side of the sample (Wan and Fell, 2002 and 2004; Muttuvel, 2008); ii) applying a constant drop pressure across the sample (Pham, 2008; Haghighi, 2012); and iii) maintaining a constant flow through the hole (Bonelli and Benahmed, 2007; Benahmed and Bonelli, 2012). The methods of the tests performed are related to technical constraints only and do not influence the erosion law of the soil, which is independent of the hydraulic conditions of the test.

In this study, tests were performed by applying a constant pressure at the inlet of the sample. Some preliminary tests were performed for each treatment to define the necessary range of applied pressure to initiate erosion by detaching soil particles. This pressure was related to the nature of the soil and the treatment product used. Table 4 provides some examples of the initial inlet pressure necessary to begin erosion for different treatment products and percentages. The erosion starting process was determined by the turbidity signal which increased when the erosion of soil particles increased.

A typical set of the test parameters monitored during a test performed on untreated soil is shown in Figure 2. The system can maintain a constant inlet pressure (Figure 2.a). At the beginning of the test, and after the clear-out of the hole from the soil particles detached during the drilling process, soil erosion increased rapidly due to the large pressure drop between the inlet and outlet of the sample (Figures 2.b and 2.c). Detachment of soil particles produced an increase in the hole diameter, creating an increase in the flow through the sample (Figure 2.d) and a progressive decrease in the pressure drop between the inlet and outlet of the sample. The evolution of the erosion rate is shown in Figure 2.e. After the increasing soil erosion phase, as also shown in the turbidity signal, the detachment of soil particles decreased progressively, likely because of the decrease in the hydraulic shear stress along the hole (Figure 2.f). The changes of the hydraulic shear stress are related to both the increase of the hole diameter and the decrease of the pressure drop between the inlet and outlet of the sample (equation 6). The test ended when the turbidity reached a lower asymptote. At the end of each test, the cell was dismantled, and the hole in the specimen was filled with liquid wax to determine the final characteristics of the eroded hole.

Theoretical model

Integration of the final shape of the hole

For all the successful tests, the cross section of the eroded hole at the end of the test was in general circular or in some cases slightly ellipsoidal. These observations lead to suggest a general theoretical model that accounts for the real final shape of the hole and accurately compute the erosion rate and hydraulic shear stress. This model was based on the two radii of the hole (a and b) to better approximate the real shape of the hole. a and b are equal for a circular hole.

The erosion rate $\dot{\varepsilon}$ (kg/s/m^2) for a given hydraulic shear stress can be expressed by the eroded soil mass (kg) per unit surface area of the hole at time t (s):

$$\dot{\varepsilon} = \frac{mass\ of\ eroded\ soil}{surface\ area\ of\ the\ hole * unit\ of time} \qquad (2)$$

Considering an ellipsoidal hole, the cross section is $S = \pi ab$ and the perimeter is $p_r = \pi\sqrt{2(a^2 + b^2)}$, where a and b are the smaller and larger radii of the ellipsoid, respectively. The erosion rate can then be expressed as follow:

$$\dot{\varepsilon} = \frac{\rho_d}{2}\sqrt{\frac{2}{a(t)^2 + b(t)^2}}\,[a(t)db + b(t)da]\,\frac{1}{dt} \qquad (3)$$

where ρ_d is the dry density of the soil (Mg/m^3); $a(t)$ and $b(t)$ are the radii of the hole (m) at time t; and db and da are the variations of the radii at the elementary time dt.

Using the principle of the equilibrium forces carried out on a volume of fluid between the inlet and outlet of the hole, the applied shear stress to the surface of the hole is related to the hydraulic gradient measured across the hole (Wan and Fell, 2002, Muttuvel, 2008). Considering the ellipsoidal shape, the hydraulic shear stress along the hole can be expressed as:

$$\tau = \frac{1}{\sqrt{2}} . \frac{\Delta P(t)}{L} . \frac{a(t).b(t)}{\sqrt{a(t)^2 + b(t)^2}} \qquad (4)$$

where L is the length of the sample (m) and $\Delta P(t)$ is the pressure drop between the inlet and outlet of the sample (Pa). To solve this equation, it is assumed that there is a unique relationship between the radius of the hole: $a = \alpha b$. The factor α is measured at the end of the test and assumed to remain constant during the test. The final radii a and b are taken as the mean values along the hole, and only specimens with a uniform shape along the hole were considered. Then, $\dot{\varepsilon}$ and τ are obtained as follows:

$$\dot{\varepsilon} = \rho_d . \sqrt{\frac{2\alpha^2}{\alpha^2 + 1}} . \frac{db}{dt} \qquad (5)$$

$$\tau = \frac{\Delta P(t)}{L} . \frac{\alpha}{\sqrt{2(\alpha^2 + 1)}} . b(t) \qquad (6)$$

Equations 5 and 6 account for the general shape of the hole. For a circular hole, a is equal to b; the coefficient α is then equal to 1.

Determination of the evolution of the radius

To compute the erosion parameters (k_{er}, τ_c), it is necessary to determine the evolution of the radius of the hole (*db*) during the test, which can be related to the soil eroded mass.

Two assumptions were made to determine the evolution of the cross-sectional shape of the hole: *i)* erosion is uniform along the hole and *ii)* the factor α relating the radii of the hole is constant. The soil eroded mass can be expressed as follows:

$$dm(t) = 2.\alpha.\pi.\rho_d.L.b(t-1).db \qquad (7)$$

where $dm(t)$ is the soil eroded mass (kg).

The soil eroded mass during time step dt is also related to the measured concentration of soil particles as follows:

$$dm(t) = c(t).q(t).dt \qquad (8)$$

where $c(t)$ is the concentration of soil particles (kg/m^3) and $q(t)$ is the water flow passing through the hole (m^3/s).

From Equations 7 and 8, db is given as follows:

$$db = \frac{c(t).q(t)}{2.\alpha.\pi.\rho_d.L} \cdot \frac{dt}{b(t-1)} \qquad (9)$$

Given the initial radius of the hole b_0, the radius at each time step can then be expressed as $[b(t) = b(t-1) + db]$.

The turbidity signal was used to determine the instantaneous concentration during the erosion process (Reddi et al., 2000; Pham, 2008; Muttuvel, 2008). The relationship between the concentration of soil and the turbidity of the effluent concentration was also calibrated. These calibrations were performed for each treatment and each percentage of treatment product. Some examples of the relationship between the soil concentration and turbidity signal are given in Figure 3. The results indicated a bilinear calibration curve for all samples. Hence, two relationships were considered for each treatment, one for each concentration range. The threshold concentration value was approximately 1 kg/m^3 and depended on the nature and percentage of treatment.

Validation of the calculation method

Figure 4 presents the final eroded diameter measured at the end of the test versus the final diameter calculated from the turbidity signal (Equation 9). The slight differences could be due to inaccuracy of initial and final drilled hole measurements and the turbidity sensor response. The results showed the relevance of the technique used to determine the hole diameter during the test using the soil detachment particles.

Impact of treatment on soil erodibility

Untreated soil

The repeatability of the erosion parameters obtained with the new HET device was verified with the untreated soil by performing several tests. Two sets of these results are shown in Figure 5. Table 5 shows the erosion parameters determined from six tests. k_{er} varies between 1.13 x 10^{-04} and 3.04 x 10^{-04} s/m, and τ_c varies between 291 and 615 Pa. This dispersion is of the same order of magnitude as has been found in previous studies. As an example, Wan and Fell (2002) found that τ_c for a clay-sandy soil varied between 85 and 327 Pa. Haghighi (2012) also found a similar range of τ_c (i.e., from 152 to 541 Pa) for a similar silty soil.

The mean values for the untreated silt are k_{er} = 2.07 x 10^{-04} s/m and τ_c= 429 Pa. The *ERI* of the tested materials is between 3.59 and 3.95; therefore, all untreated specimens are classified as having “moderately rapid” erosion according to the classification of Wan and Fell (2002).

The studied silt has a high critical shear stress compared to the values typically observed in untreated soil (Wan and Fell, 2002). This can be related to the high percentage of the fine particle fraction (< 80 μm), 99.2%, and to the compaction conditions. In fact, compaction on the wet side of optimum allows for a better rearrangement of the soil particles, than the dry side of the optimum, and reduces porosity (e.g., Benson and Daniel 1990). Compaction on the wet side (w = 17.5%) combined with the high dry density (ρ_d = 1.73 Mg/m^3) induces a dense arrangement of soil particles. This arrangement hinders the detachment of soil particles and requires a greater level of hydraulic shear stress to start the erosion. However, once this value of hydraulic shear stress is reached, the erosion rate progresses rapidly, as shown by the value of the coefficient of soil erosion (k_{er}= 2.07 x 10^{-04} s/m).

Clay treatment

Examples of the erosion law for the clay treatments are shown in Figure 6, and Table 6 summarizes the erosion characteristics for the clay-treated soil obtained from the other tests. The use of 2% kaolinite did not significantly change k_{er}; however, τ_c tended to increase and had a mean value of 607 Pa. The addition of 9% kaolinite decreased k_{er} by one order of magnitude and induced a small increase in τ_c with a mean value of 513 Pa. According to the classification of Wan and Fell (2002), the silt treated with 2% kaolinite was in the "moderately rapid" group, whereas the silt treated with 9% kaolinite became "moderately slow". Therefore, 9% kaolinite was required to significantly modify soil erodibility.

For the treatment with 2% bentonite, k_{er} is of the same order of magnitude for all samples and is approximately 5.00 x 10^{-05} s/m (Table 6) which is less than one order of magnitude less than that of the untreated soil. τ_c varies between 123 and 483 Pa, which are included within the interval of variation of τ_c for untreated silt. Thus, the silt treated with 2% bentonite is classified as "moderately slow".

The enhancement of the silt internal erosion characteristic induced by clay treatment is then characterized mainly by the reduction of the coefficient of soil erosion depending on the nature and percentage of the added product.

Lime treatment

To study the internal erosion of lime-treated silt, it was necessary to apply an inlet pressure of up to 250 kPa for 1% and 300 kPa for 3% lime to initiate soil erosion.

A typical set of results for the lime-treated silt is presented in Figure 7. Two phases can be distinguished during the test. The erosion process was initiated for a hydraulic shear stress of 926 Pa with a slope k_{er} of 3.76 x 10^{-04} s/m until a maximum erosion rate of 0.30 kg/s/m² was reached. Then, the erosion rate decreased and stopped for a hydraulic shear stress of 1,500 Pa with a mean slope of approximately 2.65 x 10^{-04} s/m. This behavior was observed with 1% and 3% lime after 7 days of curing time. τ_c at the ending phase was higher than during the starting phase (Figure 7), indicating that the soil resisted erosion more at the end of the test than at the beginning. Such behavior could be explained by the type of material used. Indeed, lime-treated soil can be considered as brittle material. The drilling is a mechanical process which may damage the brittle material by inducing small cracks. A small area of the soil around the hole could have been damaged during the drilling of the hole after the curing period. This damaged part is then the first to be easily eroded during the test, leading to a higher erodibility than the undisturbed part of the sample.

To verify this hypothesis, some tests were conducted on 3% lime-treated silt with the hole being drilled just after sample compaction. The drilled sample was then left for curing until the erosion test was performed. The results in Figure 8 showed that the effects of the drilling process were less pronounced when the drilling was made before the curing time; this observation was made for both specimens after 7 days of curing (Figure 8.a and 8.b) and after 30 days of curing (Figure 8.c and 8.d). The results also indicated that the erosion law was identical at the starting and ending phases of the test. In fact, soil drilling occurred before the beginning of the formation of the cementitious compounds that bind the soil particles. The soil is then less disturbed by the drilling just after compaction than when drilling occurs after curing. The drilling step after curing significantly modified the soil and produced different behaviors between the starting and ending phases of erosion. To examine the impact of treatment on the erosion characteristics, only the characteristics stemming from the ending phase will be considered; these characteristics correspond to the erosion of the soil that is less disturbed by the drilling process.

Some results for lime-treated soil are shown in Table 7, and examples of the erosion law are shown in Figure 9. For treatment with 1% lime, k_{er} varied between 1.09 x 10^{-04} and 2.87 x 10^{-04} s/m regardless of the curing time. For treatment with 3% lime, k_{er} varied between 1.54 x 10^{-04} and 4.52 x 10^{-04} s/m regardless of the curing time. Lime treatment increases the τ_c

of the untreated soil, yielding values of up to 1,770 Pa for 1% lime and 1,889 Pa for 3% lime. Moreover, τ_c tended to increase with curing time but not in any common progression.

The erosion rate during the test was higher for samples treated with 3% lime than for the untreated silt (Figure 9). This observation could be explained by the maximum coarse grain size in the treated soil, which is higher than the untreated soil; furthermore, during the erosion of the treated soil, the detachment of particles accompanied aggregates of larger size than for the untreated silt. It was also observed during the tests, that the erosion of lime treated soil particles often occurs by the detachment of aggregates of soil and not only individual soil particles. Hence, the erosion rate will be higher for the lime-treated silt.

The erosion of the lime-treated silt is classified as “moderately rapid,” as is that of the untreated soil, regardless of the lime percentage or curing time. The impact of the lime treatment cannot be observed in these tests because the classification of Wan and Fell (2002) does not consider the critical shear stress.

The improvement of the silt internal erosion characteristics induced by lime treatment is then characterized mainly by the increase in the critical shear stress regardless of the curing time and the percentage of the added product.

Cement treatment

Some results from the HET for the cement treatment are shown in Table 8. For 3% cement, it was necessary to apply an inlet pressure of up to 450 kPa to initiate the soil erosion; this is reflected by the high hydraulic shear stress. For most tested samples, erosion started at a hydraulic shear stress of 2,000 Pa, and the erosion was mainly independent from the curing time. For the lime-treated silt, the erosion law exhibited a different behavior between the beginning and end of the tests. Therefore, the same selection process was used to compute the erosion parameters for each step as described for the lime treatment cases. In case of treatment with 6% cement, the applied inlet pressure was more than 500 kPa, and the length of samples was reduced to 70 mm to apply a higher hydraulic shear stress. Detachment of soil particles started after 4,000 Pa for most specimens; however, the erosion law exhibited non-linear characteristics for most specimens, especially after 7 days of curing. Thus, it was difficult to compute k_{er} for some samples, and in such cases, τ_c was reported as the threshold of the hydraulic shear stress at the end of erosion.

Examples of the erosion law for cement-treated specimens are shown in Figure 10. For treatment with 3% cement, k_{er} varied between 1.13 x 10^{-04} and 1.67 x 10^{-04} s/m, regardless of the curing time. For treatment with 6% lime, k_{er} varied between 1.00 x 10^{-05} and 8.00 x 10^{-05} s/m. Furthermore, for treatment with 3% cement, τ_c varied between 2,850 and 3,619 Pa, and the curing time appeared to have no effect on the evolution of τ_c. In the case of 6% cement, τ_c varied between 4,400 and 6,800 Pa for a curing time of 1 day and reached 9,893 Pa after 7 days of curing. Thus, the erosion of cement-treated silt is classified as "moderately rapid" for 3% cement and "moderately slow" for 6% cement.

The main enhancement of the silt internal erosion characteristic induced by cement treatment is then characterized by the increase in the critical shear stress and may also result in a decrease in the coefficient of soil erosion depending on the percentage of the added product.

Discussion

Figure 11 shows the erosion characteristics (k_{er} and τ_c) obtained for both treated and untreated silt.

The addition of kaolinite induced a relatively small increase in τ_c, and the addition of bentonite did not significantly change the range of τ_c. This observation can be explained by the fact that the initial compaction states (ρ_d, w) were similar for untreated and clay-treated silt.

The addition of 9% kaolinite and 2% bentonite decreased k_{er} by one order of magnitude. The nature of the clay particles appears to have an important effect on the erosion behavior of soil. Indeed, the addition of only 2% bentonite has similar effects to the addition of 9% kaolinite. A higher percentage of clay fraction increases the resistance of sandy soils to erosion (e.g., Bennabi et al., 2012; Benahmed and Bonelli, 2012). This study showed that this trend is also valid for silty soil.

The lime treatment resulted in an increasing τ_c, even with a short curing time (1 day) (Figure 11), indicating that the increase in erosion resistance by lime treatment is a short-term effect of lime. The development of longer-term (pozzolanic) reactions for increasing the hydraulic shear stress appears to be less important. One of the short-term mechanisms responsible of these changes could be the flocculation-aggregation of soil particles caused by lime addition. The coefficient of soil erosion k_{er} maintained the same level with or without lime treatment regardless of the lime percentage or curing time, indicating that once erosion has started, the rate of soil detachment will be the same as untreated silt. This result can be explained by the detachment process of soil particles. As it was observed during the tests, the erosion of soil particles often occurs by the detachment of aggregates of soil and not only individual soil particles; this indicates that erosive forces can break more easily the weaker bonds between aggregates.

The main impact of cement treatment was the increase in τ_c in proportion to the percentage of cement (Figure 11). Furthermore, the increasing cement percentage was accompanied by a decrease in k_{er}. The enhancement of the erosion characteristics induced by cement treatment is related to the cement setting and the development of cementitious compounds, which induce strong bonds between soils particles. The detachment of soil particles becomes more difficult, making the soil more resistant to erosion. When treated with 3% cement, this improvement came in early ages of curing time, and no further significant modification was observed until 30 days. At higher percentages of cement (6%), an increase in the critical shear stress was obtained with increasing curing time. This behavior could be related to the soil-cement setting time, which may be longer for a higher amount of cement treatment.

Conclusion

The main objective of this paper was to study the impact of soil treatment on the internal erosion resistance of treated compacted silt. A new enhanced HET device was developed to determine the erosion characteristics of treated materials. A modified interpretation method that considered the final shape of the eroded hole has been proposed.

The results showed that the studied silt had a higher critical shear stress compared to the values typically observed in the untreated soil. This higher critical shear stress was primarily caused by the compaction conditions on the wet side of the optimum water content. However, the mean coefficient of soil erosion was 2.07×10^{-04} s/m, which may accelerate detachment due to erosion once it has begun. The solution to this issue could be the treatment of soil by adding clay, lime or cement. The following conclusions can be made based on the results obtained:

- The use of clay soil as a treatment product reduces the erosion rate of soil particles. This effect is related to the nature of the clay, and the use of bentonite further reduces the coefficient of soil erosion than the use of kaolinite at the same percentage.
- Lime treatment increases the internal erosion resistance of soil by increasing the critical shear stress. This effect is similar to either 1 or 3% lime treatment and occurs rapidly, with no significant change with increased curing time up to 30 days.
- Cement treatment increases the critical shear stress, and the increase in erosion resistance is proportional to the percentage of cement used. A high percentage of cement will also provide a smaller coefficient of soil erosion. The enhancement occurs

rapidly for 3% cement, whereas higher percentages require additional curing time to yield greater erosion resistance.

Additional works are required to relate the evolution of erosion characteristics to the microstructure of the treated soil which may give more information about the factors responsible of the changes of the erosion characteristics.

Although the short-term effects seemed to be positive, the use of these treatments for hydraulic earth structures should consider their long-term behavior. In fact, such products require specific studies to assess the evolution of these parameters over time when the structures are submitted to climatic conditions, which can affect the sustainability of treatments and decrease their initial performances. The impact of these different treatment products on other hydro-mechanical parameters (e.g., hydraulic conductivity, unconfined compression strength) of the tested soil should also be considered in the framework of the selection of the most cost effective treatment product.

Acknowledgment

The authors would like to thank S. Bonne, E. Lavallée and T. Le Borgne from DTP - Bouygues Construction - France for their valuable support of this study.

References

Al-Amoudi, O.S.B., (2002). Characterization and chemical stabilization of Al-Qurayyah sabkha soil. Journal of Materials in Civil Engineering, vol. 14, No 6, 478-484.

ASTM D 4647-98, (1998). Standard Test Method for Identification and Classification of Dispersive Clay Soils by the Pinhole Test. American Society For Testing and Materials, West Conshohocken, 11 p.

ASTM-D 698-98, (1998). Standard Test Method for Laboratory Compaction Characteristics of Soil Using Standard Effort. American Society For Testing and Materials, West Conshohocken, 8 p.

Attom, M., (2012). The effect of compaction condition and initial water content on soil erosion. International Conference on Scour and Erosion, ICSE6 Paris, 49-56.

Bell, F.G., (1996). Lime stabilization of clay minerals and soils. Engineering Geology, vol. 42, 223-237.

Bellezza, I., Fratalochi, E., (2006). Effectiveness of cement on hydraulic conductivity of compacted soil-cement mixtures. Ground Improvement, vol. 10, No 2, 77-90.

Benahmed, N., Bonelli, S., (2007). Etude expérimentale de l'érosion interne d'une kaolinite. 25e Rencontres de l'AUGC 2007, Bordeaux, France, 8 p.

Benahmed, N., Bonelli, S., (2012). Investigation concentrated leak erosion behaviour of cohesive soils by performing hole erosion tests. European Journal of Environmental and Civil Engineering, vol. 16, No 1, 43-58.

Bennabi, A., Karoui, T., Benamar, A., Wang, H.Q., (2012). Some elements of comparison between two laboratory devices for soil erosion testing. International Conference on Scour and Erosion, ICSE6 Paris, 1089-1096.

Benson, C.H., Daniel, D.E., (1990). Influence of clods on hydraulic conductivity of compacted clay. Journal of Geotechnical Engineering, vol. 116, No 8, 1231-1247.

Brandl, H., (1981). Alteration of soil parameters by stabilization with lime, Proceedings of the 10th International Conference on Soil Mechanics and foundation Engineering, Stockholm, vol. 3, 587-594.

Chapuis, R.P., (2002).The 2000 R.M. Hardy Lecture: Full-scale hydraulic performance of soil-bentonite and compacted clay liners. Canadian Geotechnical Journal, vol. 39, No 2, 417-439.

Chevalier, C., Haghighi, I., Herrier, G., (2012). Resistance to erosion of lime treated soils: a complete parametric study in laboratory. International Conference on Scour and Erosion, ICSE6 Paris, 1065-1072.

Cuisinier, O., Auriol, J.C., Le Borgne, T., Denelle, D., (2011). Microstructure and hydraulic conductivity of a compacted lime-treated soil. Engineering Geology, vol. 123, 187-193.

Eades, J.L., Grim, R.E., (1966). A quick test to determine lime requirements for lime stabilization. Highway Research Board Bulletin, vol. 139, 61-72.

Farrar, J.A., Torres, R.L., Erdogan, Z., (2007). Bureau of reclamation erosion testing for evaluating piping and internal erosion of dams. Geotechnical Special Publication, vol. 167, No 3, 22-31.

Fell, R., Wan, C.F., Cyganiewicz, J., Foster, M., (2003). Time for development of internal erosion and piping in embankment dams. Journal of Geotechnical and Geoenviromental Engineering, vol. 129, No 4, 2003, 307-314.

Haghighi, I., (2012). Caractérisation des phénomènes d'érosion et de dispersion des sols : développement d'essais et applications pratiques. PhD thesis, Ecole Nationale des Ponts et Chaussées, Paris, France, 202 p.

Haghighi, I., Chevalier, C., Duc, M., Guédon, S., Reiffsteck, P., (2013). Improvement of hole erosion test and results on reference soils. Journal of Geotechnical and Geoenvironmental engineering, vol. 139, No 2, 330–339.

Herrier, G., Chevalier, C., Froumentin, M., Cuisinier, O., Bonelli, S., Fry, J.J., (2012). Lime treated soil as an erosion-resistant material for hydraulic earthen structures. International Conference on Scour and Erosion, ICSE6 Paris, 585-592.

Indraratna, B., Muttuvel, T., Khabbaz, H., (2009). Modelling the erosion rate of chemically stabilized soil incorporating tensile force-deformation charcacteristics. Canadian Geotechnical journal, vol. 46, 57-68.

Le Runigo, B., Cuisinier, O., Cui, Y.-J., Ferber, V., Deneele, D., (2009). Impact of initial state on the fabric and permeability of a lime-treated silt under long-term leaching. Canadian Geotechnical Journal, vol. 46, 1243-1257.

Lefebvre, G., Rohan, K., Douville, S., (1985). Erosivity of natural intact structured clay: evaluation. Canadian Geotechnical Journal, vol. 22, 508-517.

Lim, S.S., (2006). Experimental investigation of erosion in variably saturated clay soils. PhD thesis, University of New South Wales, Australia. 171 p.

Luthi, M., Fannin, R.j., Milar, R.G., (2012). A modified hole erosion test (HET-P) device. Geotechnical Testing Journal, vol. 35, No 4, 660-664.

McCallister, L.D., Petry, T.M., (1991). Physical property changes in a lime-treated expansive clay caused by leaching. Transportation Research Record, vol. 1295, 37-44.

Mitchell, J.K., Hooper, D. R., Campanella, R. G. (1965). Permeability of compacted clays. Journal of the Soil Mechanics and Foundation Division, vol. 91, No sm, 41-65.

Muttuvel, T., (2008). Erosion rate of chemically stabilized soils incorporating tensile stress-deformation behaviour. PhD thesis, University of Wollongong, Australia.202 p.

Pham, T.L., (2008). Erosion et dispersion des sols argileux par un fluide. PhD thesis, Ecole Nationale des Ponts et Chaussées, Paris, France, 232 p.

Reddi, L.N., Lee, I.M., Bonala, M.V.S., (2000). Comparison of internal and surface erosion using flow pump tests on a sand-kaolinte mixture. Geotechnical Testing Journal, vol. 23, 116-122.

Rohan, K., Lefebvre, G., Douville, S., Milette, J.P., (1986). A new technique to evaluate erosivity of cohesive material. Geotechnical Testing Journal, vol. 9, 87-92.

Sariosseiri, F., Muhunthan, B., (2009). Effect of cement treatment on geotechnical properties of some Washington state soils. Engineering Geology, vol. 104, 119-125.

SETRA-LCPC, (2000). Traitement des sols à la chaux et/ou aux liants hydrauliques (GTS) - Application à la réalisation des remblais et des couches de forme. Technical manual, 240 p.

Sherard, J.L., Dunnigan, L.P., Decker, R.S., Steele, E.F., (1976). Pinhole test for identifying dispersive soils. Journal of Geotechnical Engineering Division, vol. 102, No GT1, 69-85.

Sivapillaiah, P.V., Sridharan, A., Stalin, V.K. (2000). Hydraulic conductivity of bentonite-sand mixtures. Canadian Geotechnical Journal, vol. 37, 406-413.

Wahl, T., (2010). A comparison of the hole erosion test and jet erosion test. Joint Federal Interagency Conference on Sedimentation and Hydrologic Modeling, Las Vegas 2010, 11 p.

Wan, C.F., Fell, R., (2002). Investigation of internal erosion and piping of soils in embankment dams by the slot erosion test and the hole erosion test. UNICIV Report, No R-412, 358 p.

Wan, C.F., Fell, R., (2004). Investigation of rate of erosion of soils in embankment dams. Journal of Geotechnical and Geoenviromental Engineering, vol. 130, No 4, 373-380.

Watabe, Y., Leroueil, S., Le Bihan, J–P., (2000). Influence of compaction conditions on pore-size distribution and saturated hydraulic conductivity of a glacial till. Canadian Geotechnical Journal, vol. 37, 1184-1194.

Tables

Table 1: Method of the classification of soils based on their erodibility (Wan and Fell, 2002).

Table 2: Physical and geotechnical properties of the studied soil.

Table 3: Optimum Proctor compaction characteristics for silt treated with different products and the compaction characteristics for the HET samples.

Table 4: Example of the range of the initial applied inlet pressures for different treatments.

Table 5: Erosion characteristics for the untreated silt calculated from 6 tests.

Table 6: Impact of clay treatments on the erosion characteristics of the studied silt.

Table 7: Erosion characteristics of lime-treated silt calculated from several tests after 1, 7 and 30 days.

Table 8: Erosion characteristics for cement-treated silt calculated from several tests after 1, 7 and 30 days.

Figures

Figure 1: Schematic of the enhanced HET testing cell.

Figure 2: Example results for a HET performed on a sample of untreated silt.
a) pressure applied at the inlet of the sample.
b) pressure drop between the inlet and outlet of the sample.
c) turbidity signal of the effluent.
d) flow through the sample.
e) erosion rate.
f) hydraulic shear stress.

Figure 3: Relationship between the soil concentration and turbidity signal.
a) concentration interval [0 - 1.5 kg/m^3].
b) concentration interval [0 - 15 kg/m^3].
The best fit line is drawn for each treatment.

Figure 4: Representation of the calculated and measured diameter at the end of the different tests.

Figure 5: Two examples of erosion law for the untreated silt.

Figure 6: Impact of clay treatment on the erosion characteristics of silt.

The lines represent the erosion law drawn from the best fit line for the selected data of each treatment.

Figure 7: Example of the erosion law for lime-treated silt (1%) with 7 days of curing.

Figure 8: Impact of the drilling on the erosion law of 3% lime-treated soil.
a) drilling after 7 days of curing
b) drilling before 7 days of curing
c) drilling after 30 days of curing
d) drilling before 30 days of curing

Figure 9: Examples of the erosion law for lime-treated samples.

The lines represent the erosion law drawn from the best fit line for the selected data of each treatment.

Figure 10: Example of the erosion law for cement-treated silt.

The lines represent the erosion law drawn from the best fit line for the selected data of each treatment.

Figure 11: Effect of treatment on the erosion characteristics of the studied silt.

The vertical small bar refers to samples where the coefficient of soil erosion was calculated at the starting phase only.

Table 1: Method of the classification of soils based on their erodibility (Wan and Fell, 2002).

Group number	Erosion Rate Index (*ERI*)	Description
1	<2	Extremely rapid
2	2 – 3	Very rapid
3	3 – 4	Moderately rapid
4	4 – 5	Moderately slow
5	5 – 6	Very slow
6	>6	Extremely slow

Table 2: Physical and geotechnical properties of the studied soil.

Soil properties	Value
Liquid limit (%)	28.5
Plastic limit (%)	20.5
Plasticity index (%)	8.0
Passing sieve 80 µm (%)	99.2
Clay size content (<2 µm) (%)	6.0
Specific gravity Gs (−)	2.64

Table 3: Optimum Proctor compaction characteristics for silt treated with different products and the compaction characteristics for the HET samples.

Types of treatment	Notation	Optimum Proctor compaction characteristics		Compaction characteristics for the HET samples	
		ρ_{dmax} (Mg/m^3)	w_{OMC} (%)	ρ_d (Mg/m^3)	w (%)
Silt	S	1.82	15.0	1.73	17.5
+ 2% kaolinite	SK 2%	1.80	15.5	1.73	18.0
+ 9% kaolinite	SK 9%	1.79	15.8	1.74	18.3
+ 2% bentonite	SB 2%	1.78	15.3	1.74	17.8
+ 1% lime	SL 1%	1.75	17.5	1.70	20.0
+ 3% lime	SL 3%	1.73	17.5	1.68	20.0
+ 3% cement	SC 3%	1.81	15.0	1.75	17.5
+ 6% cement	SC 6%	1.82	15.0	1.75	17.5

Table 4: Example of the range of the initial applied inlet pressures for different treatments.

Type of treatments	**Range of initial applied pressure (kPa)**
Silt	70-80
+ 2% kaolinite	70-80
+ 9% kaolinite	100-120
+ 2% bentonite	75-85
+ 1% lime	150-250
+ 3% lime	200-300
+ 3% cement	400-500
+ 6% cement	500-650

Table 5: Erosion characteristics for the untreated silt calculated from 6 tests.

Test	**k_{er} (s/m)**	**τ_c(Pa)**	**Mean values**	
			k_{er}(s/m)	**τ_c(Pa)**
1	2.58 x 10^{-04}	391	2.07 x 10^{-04}	429
2	2.16 x 10^{-04}	389		
3	2.22 x 10^{-04}	398		
4	1.13 x 10^{-04}	491		
5	3.04 x 10^{-04}	615		
6	1.30 x 10^{-04}	291		

Table 6: Impact of clay treatments on the erosion characteristics of the studied silt.

Test	Nature of treatment	k_{er} (s/m)	τ_c(Pa)	Mean values	
				k_{er}(s/m)	τ_c(Pa)
1	+ 2% kaolinite	1.54 x 10^{-04}	586	1.99 x 10^{-04}	607
2		2.68 x 10^{-04}	754		
1	+ 9% kaolinite	4.62 x 10^{-05}	668	6.92 x 10^{-05}	530
2		8.10 x 10^{-05}	391		
3		5.05 x 10^{-05}	519		
1	+ 2% bentonite	5.66 x 10^{-05}	357	5.62 x 10^{-05}	316
2		5.71 x 10^{-05}	511		
3		5.13 x 10^{-05}	123		

Table 7: Erosion characteristics of lime-treated silt calculated from several tests after 1, 7 and 30 days.

Test	**Nature of treatment (curing time)**	**Erosion characteristics from the ending phase**		**Mean values**	
		k_{er}**(s/m)**	τ_c**(Pa)**	k_{er}**(s/m)**	τ_c**(Pa)**
1	**+ 1% lime (1d)**	1.20 x 10^{-04}	618	1.25 x 10^{-04}	745
2		2.62 x 10^{-04}	836		
1	**+ 1% lime (7d)**	2.87 x 10^{-04}	1725	2.63 x 10^{-04}	1660
2		2.35 x 10^{-04}	1770		
1	**+ 1% lime (30d)**	2.53 x 10^{-04}	1538	2.11 x 10^{-04}	1279
2		1.09 x 10^{-04}	963		
1	**+ 3% lime (1d)**	2.47 x 10^{-04}	1409	2.24 x 10^{-04}	1200
1	**+ 3% lime (7d)**	1.75 x 10^{-04}	1863	2.46 x 10^{-04}	1707
2		4.52 x 10^{-04}	1889		
3		2.15 x 10^{-04}	1567		
4		2.28 x 10^{-04}	1522		
5		3.07 x 10^{-04}	1648		
6		1.81 x 10^{-04}	1608		
1	**+ 3% lime (30d)**	2.27 x 10^{-04}	1035	1.71 x 10^{-04}	1362
2		1.78 x 10^{-04}	1197		
3		1.68 x 10^{-04}	1 845		
4		2.42 x 10^{-04}	1 365		
5		1.67 x 10^{-04}	1 405		

Table 8: Erosion characteristics for cement-treated silt calculated from several tests after 1, 7 and 30 days.

NE: not established at the ending of the erosion phase.

Test	Nature of treatment (curing time)	Erosion characteristics from the ending phase		Mean values	
		k_{er}(s/m)	τ_c(Pa)	k_{er}(s/m)	τ_c(Pa)
1	+ 3% cement (1d)	1.13×10^{-04}	2850	1.13×10^{-04}	2850
2		NE	2850		
1	+ 3% cement (7d)	1.22×10^{-04}	2520	1.31×10^{-04}	2985
2		1.47×10^{-04}	3619		
1	+ 3% cement (30d)	1.43×10^{-04}	2531	1.47×10^{-04}	2886
2		1.67×10^{-04}	3150		
1	+ 6% cement (1d)	8.00×10^{-05}	6475	4.83×10^{-05}	5891
2		1.00×10^{-05}	6800		
1	+ 6% cement (7d)	NE	9734	NE	9814
2		NE	9893		

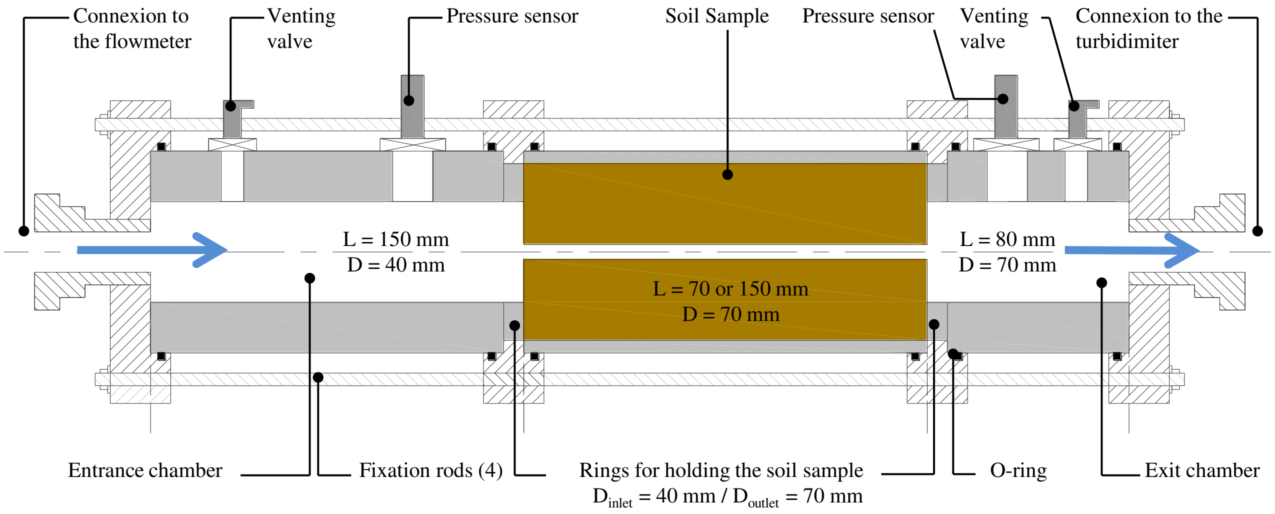
Connexion to the flowmeter
Venting valve
Pressure sensor
Soil Sample
Pressure sensor
Venting valve
Connexion to the turbidimiter
L = 150 mm
D = 40 mm
L = 80 mm
D = 70 mm
L = 70 or 150 mm
D = 70 mm
Entrance chamber
Fixation rods (4)
Rings for holding the soil sample
D_{inlet} = 40 mm / D_{outlet} = 70 mm
O-ring
Exit chamber

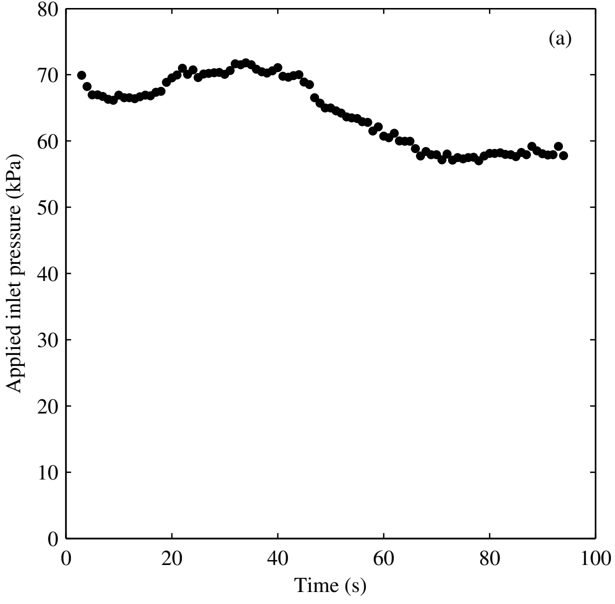
(a)
Applied inlet pressure (kPa)
0
10
20
30
40
50
60
70
80
Time (s)
0
20
40
60
80
100

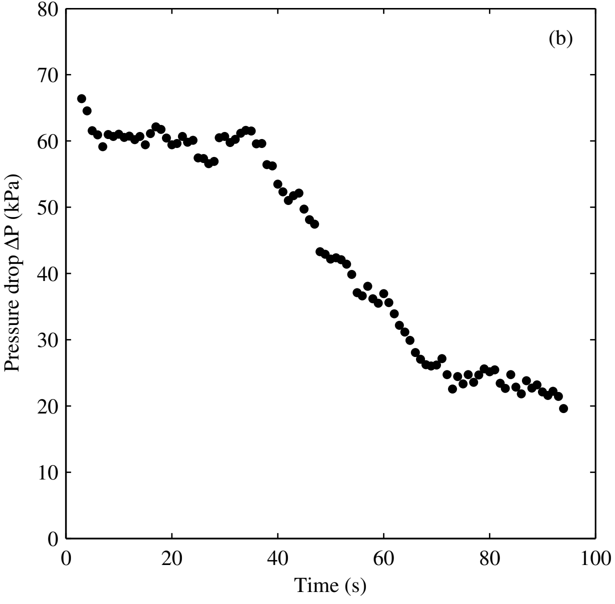
(b)
Pressure drop ΔP (kPa)
Time (s)
0
10
20
30
40
50
60
70
80
0
20
40
60
80
100

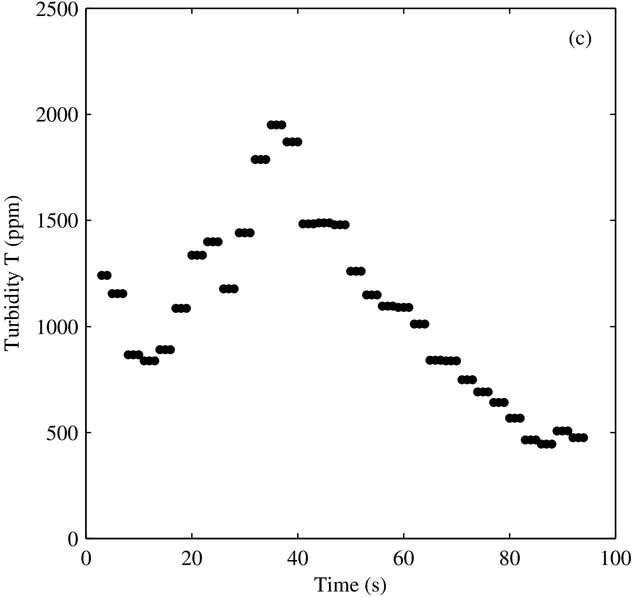
(c)
Turbidity T (ppm)
Time (s)
0
500
1000
1500
2000
2500
0
20
40
60
80
100

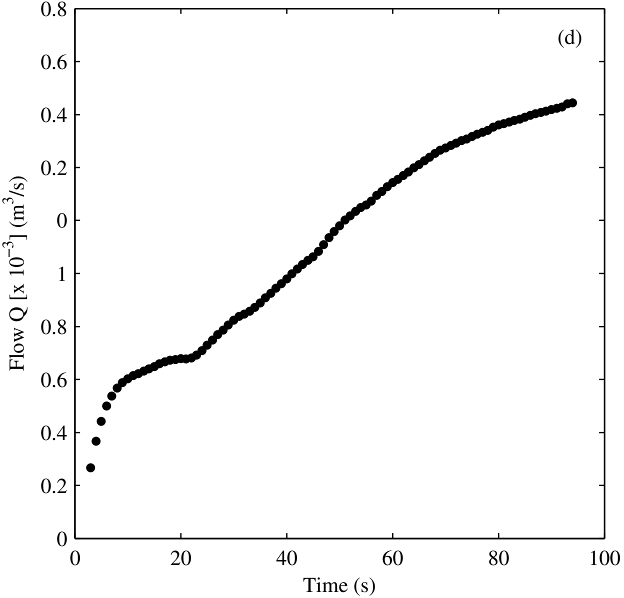
(d)
Flow Q [x 10^{-3}] (m^3/s)
Time (s)
0
20
40
60
80
100
0
0.2
0.4
0.6
0.8
1
0
0.2
0.4
0.6
0.8

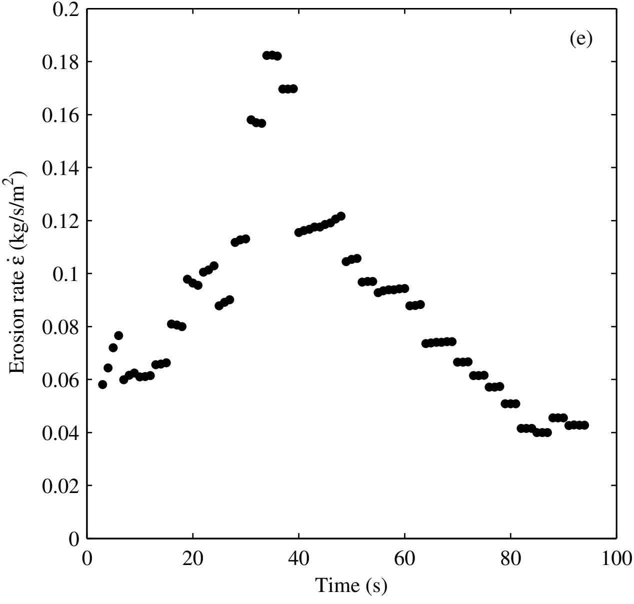
(e)
Erosion rate $\dot{\varepsilon}$ (kg/s/m^2)
0
0.02
0.04
0.06
0.08
0.1
0.12
0.14
0.16
0.18
0.2
Time (s)
0
20
40
60
80
100

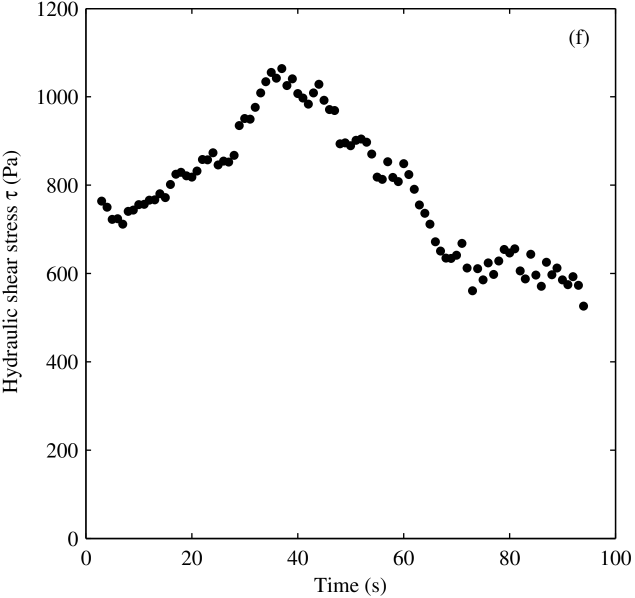
(f)
Hydraulic shear stress τ (Pa)
Time (s)
0
200
400
600
800
1000
1200
0
20
40
60
80
100

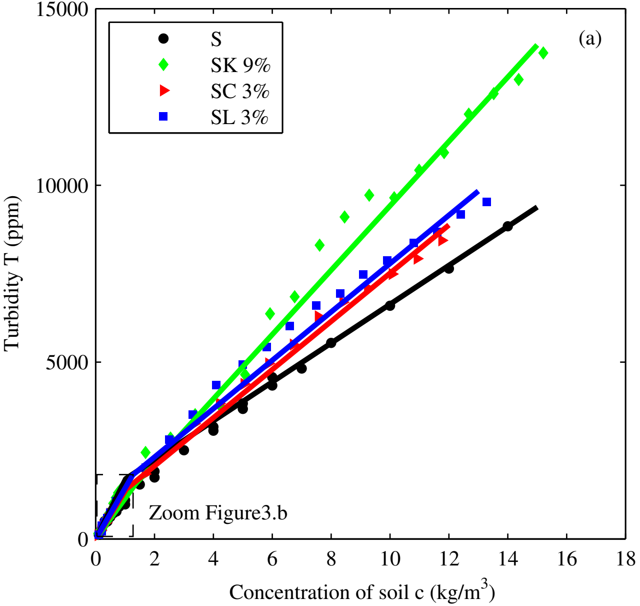
15000
10000
5000
0
0
2
4
6
8
10
12
14
16
18
Turbidity T (ppm)
Concentration of soil c (kg/m^3)
S
SK 9%
SC 3%
SL 3%
(a)
Zoom Figure3.b

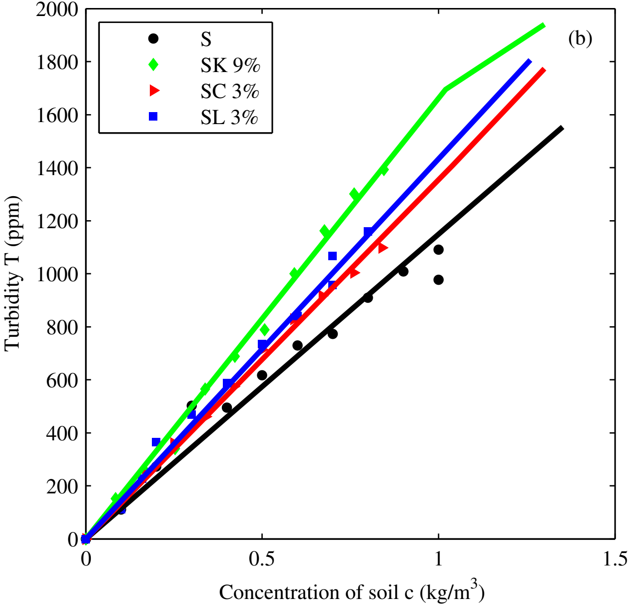
(b)
S
SK 9%
SC 3%
SL 3%
Turbidity T (ppm)
2000
1800
1600
1400
1200
1000
800
600
400
200
0
0
0.5
1
1.5
Concentration of soil c (kg/m^3)

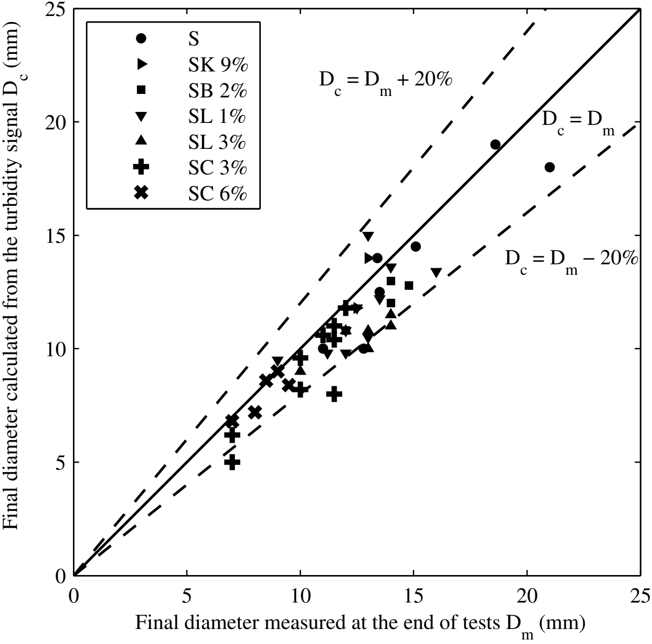
S
SK 9%
SB 2%
SL 1%
SL 3%
SC 3%
SC 6%
$D_c = D_m + 20\%$
$D_c = D_m$
$D_c = D_m - 20\%$
Final diameter calculated from the turbidity signal D_c (mm)
Final diameter measured at the end of tests D_m (mm)
0
5
10
15
20
25
0
5
10
15
20
25

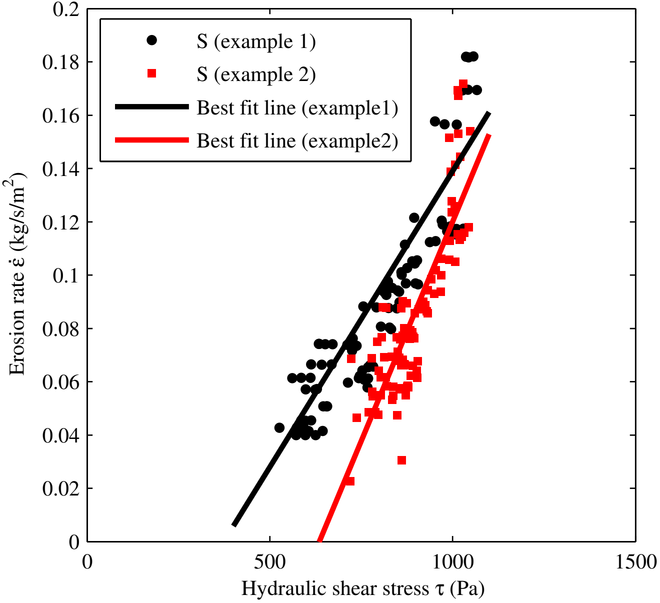
0.2
0.18
0.16
0.14
0.12
0.1
0.08
0.06
0.04
0.02
0
Erosion rate ε̇ (kg/s/m^2)
0
500
1000
1500
Hydraulic shear stress τ (Pa)
● S (example 1)
■ S (example 2)
Best fit line (example1)
Best fit line (example2)

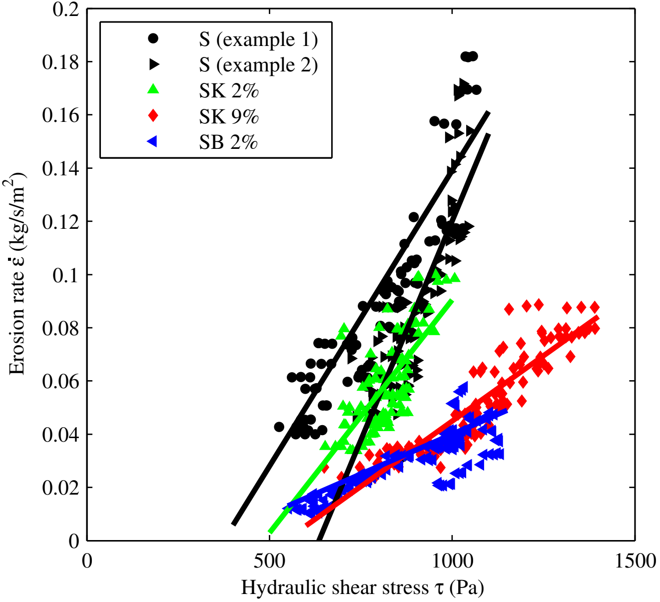

0.2
0.18
0.16
0.14
0.12
0.1
0.08
0.06
0.04
0.02
0
0
500
1000
1500
Erosion rate ε̇ (kg/s/m²)
Hydraulic shear stress τ (Pa)
S (example 1)
S (example 2)
SK 2%
SK 9%
SB 2%

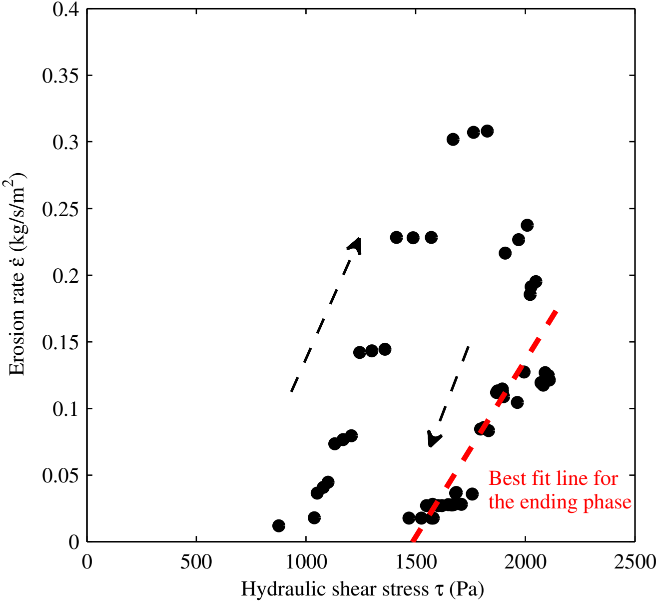
Erosion rate $\dot{\varepsilon}$ (kg/s/m^2)
0.4
0.35
0.3
0.25
0.2
0.15
0.1
0.05
0
0
500
1000
1500
2000
2500
Hydraulic shear stress τ (Pa)
Best fit line for
the ending phase

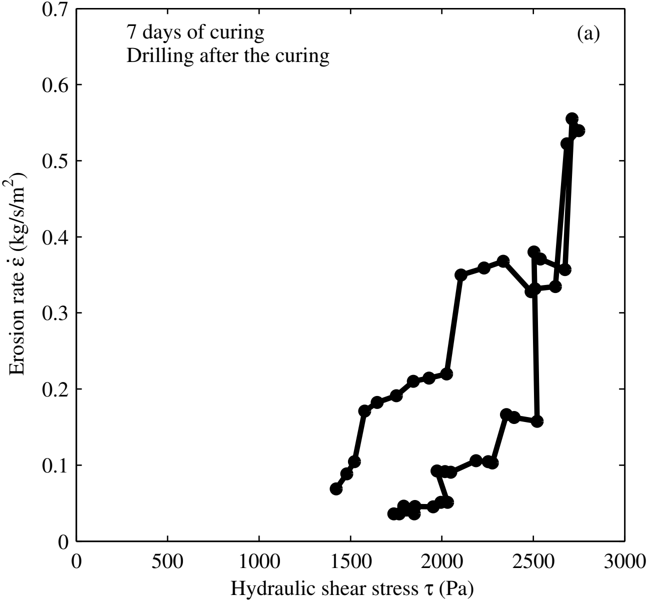

7 days of curing
Drilling after the curing
(a)
Erosion rate $\dot{\varepsilon}$ (kg/s/m^2)
Hydraulic shear stress τ (Pa)
0
0.1
0.2
0.3
0.4
0.5
0.6
0.7
0
500
1000
1500
2000
2500
3000

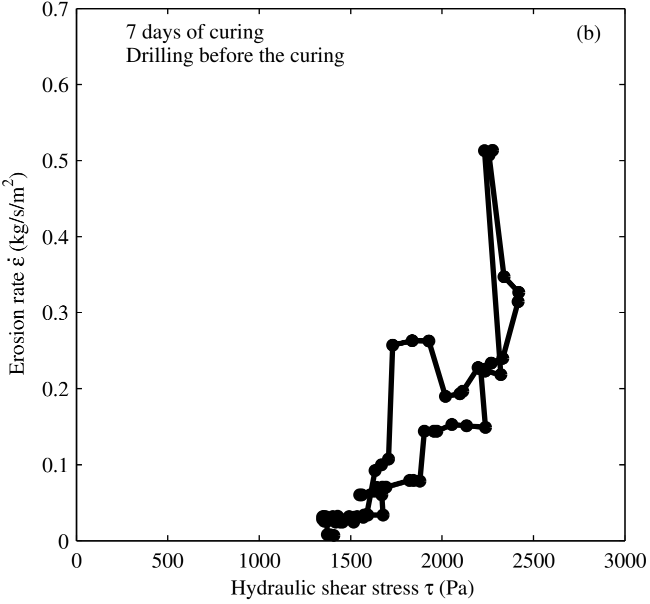
0.7
0.6
0.5
0.4
0.3
0.2
0.1
0
Erosion rate $\dot{\varepsilon}$ (kg/s/m^2)
0
500
1000
1500
2000
2500
3000
Hydraulic shear stress τ (Pa)
7 days of curing
Drilling before the curing
(b)

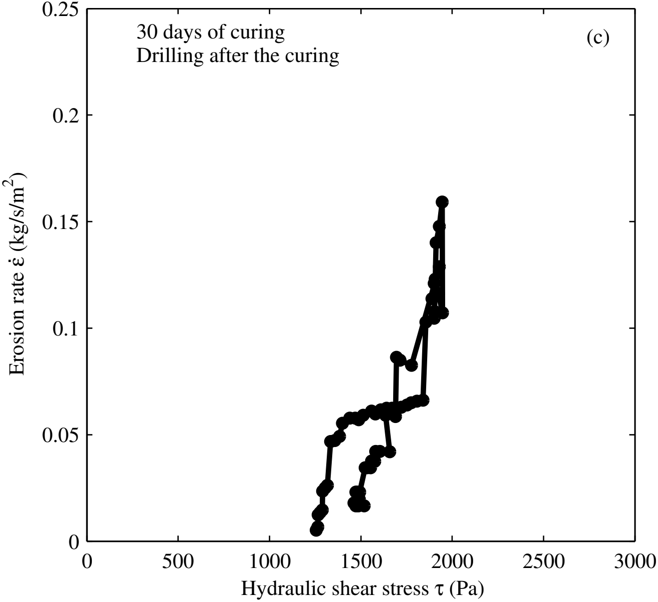
30 days of curing
Drilling after the curing
(c)
Erosion rate $\dot{\varepsilon}$ (kg/s/m^2)
0.25
0.2
0.15
0.1
0.05
0
0
500
1000
1500
2000
2500
3000
Hydraulic shear stress τ (Pa)

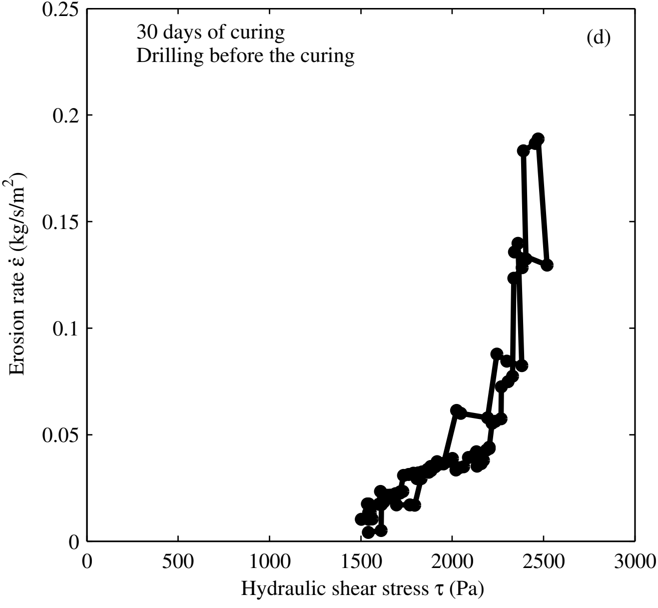

30 days of curing
Drilling before the curing
(d)
Erosion rate $\dot{\varepsilon}$ (kg/s/m^2)
0.25
0.2
0.15
0.1
0.05
0
0
500
1000
1500
2000
2500
3000
Hydraulic shear stress τ (Pa)

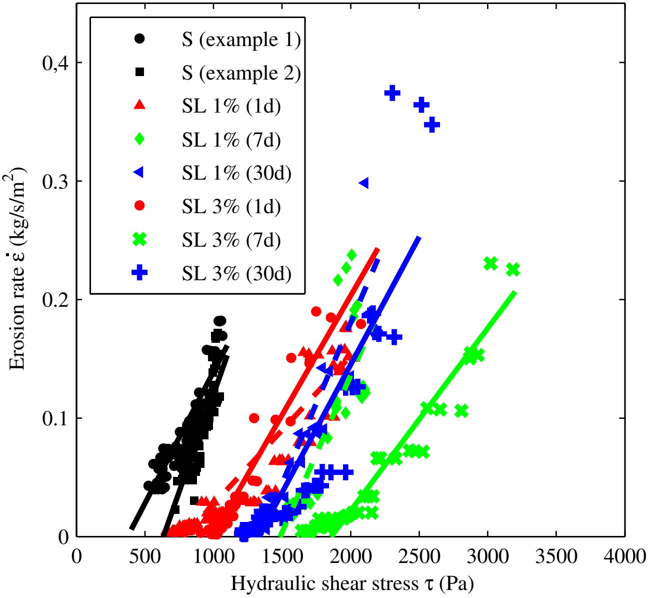
S (example 1)
S (example 2)
SL 1% (1d)
SL 1% (7d)
SL 1% (30d)
SL 3% (1d)
SL 3% (7d)
SL 3% (30d)
Erosion rate ε̇ (kg/s/m²)
0
0.1
0.2
0.3
0,4
Hydraulic shear stress τ (Pa)
0
500
1000
1500
2000
2500
3000
3500
4000

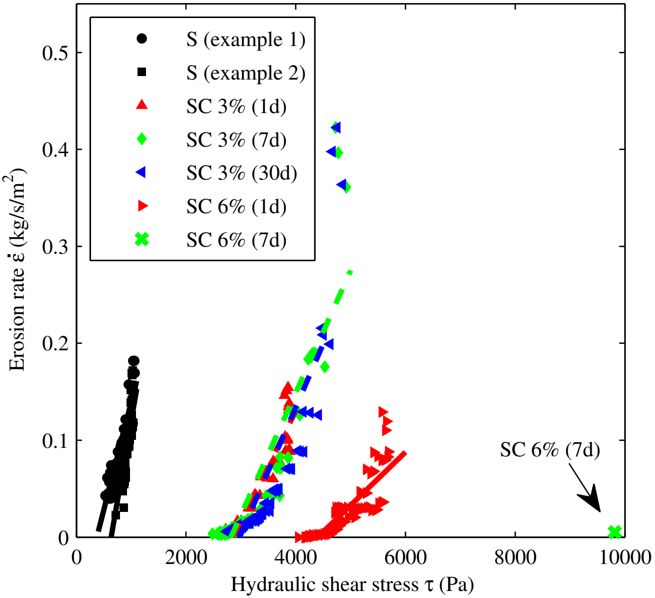

S (example 1)
S (example 2)
SC 3% (1d)
SC 3% (7d)
SC 3% (30d)
SC 6% (1d)
SC 6% (7d)
SC 6% (7d)
Erosion rate ε̇ (kg/s/m²)
Hydraulic shear stress τ (Pa)
0
0.1
0.2
0.3
0.4
0.5
0
2000
4000
6000
8000
10000

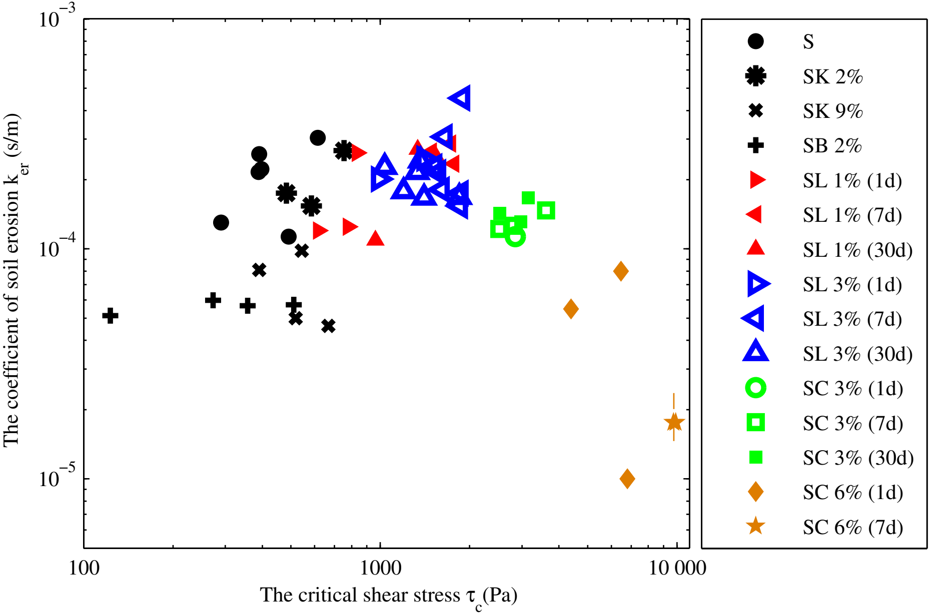
10^−3
10^−4
10^−5
100
1000
10 000
The coefficient of soil erosion k_er (s/m)
The critical shear stress τ_c (Pa)
S
SK 2%
SK 9%
SB 2%
SL 1% (1d)
SL 1% (7d)
SL 1% (30d)
SL 3% (1d)
SL 3% (7d)
SL 3% (30d)
SC 3% (1d)
SC 3% (7d)
SC 3% (30d)
SC 6% (1d)
SC 6% (7d)